AIAS – ASSOCIAZIONE ITALIANA PER L'ANALISI DELLE SOLLECITAZIONI
XXXIX CONVEGNO NAZIONALE, 7-10 SETTEMBRE 2010, MARATEA

AIAS 2010 - 057

MULTI OBJECTIVE OPTIMISATION BY MEANS OF MESH MORPHING: APPLICATION OF RBF MORPH TO A FSAE CAR AIRBOX DESIGN

E. Abbasciano, M.E. Biancolini, M. Urbinati

Università di Roma "Tor Vergata", Dipartimento di Meccanica,
Via del Politecnico, 1 – 00133 Roma, e-mail: emanuel_abbasciano@libero.it
biancolini@ing.uniroma2.it, urbinati@ing.uniroma2.it

Sommario
In questa memoria viene presentata un'applicazione di un metodo innovativo per l'ottimizzazione di forma mediante mesh morphing: l'ottimizzazione strutturale e fluidodinamica dell'airbox di una vettura FSAE. La soluzione in uso montata sulla vettura FSAE TV-460R (STV Team, Università di Roma Tor Vergata) manifesta una forte disomogeneità di carica fra i cilindri interni ed esterni. Si è pertnato resa necessaria l'ottimizzazione di una nuova soluzione in grado di minimizzare tale sbilanciamento di carica mantenendo la massima efficienza volumetrica possibile.
Tale ottimizzazione è stata possibile grazie all'uso delle simulazioni CFD (Fluent) e FEM (Nastran) rese parametriche mediante il software di mesh morphing RBF Morph.

Abstract
In this paper a new mesh morphing approach for shape optimisation is presented through an industrial application: the structural and fluid dynamic optimization of a FSAE car airbox. The current configuration of the inlet system of the FSAE car TV-460R (STV Team, University of Rome Tor Vergata) suffers a consistent charging imbalance between internal and external runners. A new design needs to be optimised to find the optimal shape that minimize charging imbalance whilst preserving an overall volumetric efficiency of the engine.
This challenging optimization task was made possible thanks to numerical CFD (Fluent) and FEM (Nastran) simulations parameterised by means of the mesh morphing tool RBF Morph.

1. INTRODUCTION

Shape optimization is a very important topic especially in problems where the motion of a fluid has an important impact over performances. In fact, a slight shape modification can dramatically affect the behaviour of a component that interacts with the fluid itself. CFD can give an important aid to drive the design of such critical components but a true parametric CFD solver, suitable for optimization, is still missing on the market, especially when large problems need to be handled.
Despite shape parameterization is available in the CAD model, used as starting point for CFD model generation, the complex chain that allows to obtain a reliable CFD grid is very difficult to manage. As such, parametric properties and geometric features of the original CAD model are usually lost in the final mesh.
The effects of slight modifications can be addressed acting at final level of the complex aforementioned chain: the CFD mesh. In fact required modifications can be introduced by morphing the surface mesh at the boundary of fluid mesh and propagating such deformations inside the domain by means of a smoother. The original mesh topology is preserved but the final quality of the mesh depends on the action of surface morpher and fluid smoother.

In this paper the new morphing product RBF Morph [1,2] is presented starting from the exposition of the background theory of Radial Basis Functions used for the implementation of the numerical kernel of the software.
To better understand how RBF Morph can be used for industrial cases, a practical application is considered in the present study: the optimization of the airbox used for the engine of a Formula SAE car [3,4].

2. RBF MORPH

The new product RBF Morph, an integrated system for morphing and shape optimization tailored for the CFD solver ANSYS Fluent, is herein presented. RBF Morph is fully integrated in the CFD solving process and combines a very accurate control of the geometrical parameters with an extremely fast mesh deformation. RBF Morph is the result of the joint between academic state-of-the-art research and top-level industrial needs. In the present implementation, the morpher has been tailored to ANSYS Fluent. However, the kernel of the software represents the most sophisticated component, and could be adapted to different tasks or stand-alone work.

2.1 The aim

The aim of the RBF Morph is to perform fast mesh morphing using a mesh-independent approach based on state-of-the-art RBF (Radial Basis Functions) techniques.
The use of RBF Morph allows the CFD user to perform shape modifications, compatible with the mesh topology, directly in the solving stage, just adding one single command line in the input file.
The most important requirements are:

- mesh-independent solution;
- parallel morphing of the grid;
- large size models (many millions of cells) must be morphed in a reasonable short time
- management of every kind of mesh element type (tetrahedral, hexahedral, polyhedral, prismatic, hexcore, non-conformal interfaces, etc.).

The final goal is to perform parametric studies of component shapes and positions typical of the fluid-dynamic design like:

- design Developments;
- multi-configuration studies;
- sensitivity Studies;
- DOE (Design Of Experiment);
- optimization.

2.2 Background

A system of radial functions is used to produce a solution for mesh movement/morphing, from a list of source points and their displacements [1,2]. This approach is valid for both surface shape changes and volume mesh smoothing.
Radial basis were born as an interpolation tool for scattered data and consist of a very powerful tool because they are able to interpolate everywhere in the space a function defined at discrete points giving the exact value at original points. The behaviour of the function between points depends on the kind of basis adopted.
The radial function can be fully or compactly supported, in any case a polynomial corrector is added to guarantee compatibility for rigid modes. Typical radial functions are reported in Table 1.

Table1: radial basis functions.

Radial Basis Function	$\phi(r)$
Spline type (R_n)	$\lvert r\rvert^n$, n odd
Thin plate spline (TPS_n)	$\lvert r\rvert^n \log\lvert r\rvert$, n even
Multiquadric(MQ)	$\sqrt{1+r^2}$
Inverse multiquadric (IMQ)	$\frac{1}{\sqrt{1+r^2}}$
Inverse quadratic (IQ)	$\frac{1}{1+r^2}$
Gaussian (GS)	e^{-r^2}

As will be shown in detail, a linear system (of order equal to the number of source point introduced) need to be solved for coefficients calculation. Once the unknown coefficients are calculated, the motion of an arbitrary point inside or outside the domain (interpolation/extrapolation) is expressed as the summation of the radial contribution of each source point (if the point falls inside the influence domain). Details of the theory need to be given using some equations. An interpolation function composed by a radial basis and a polynomial is defined as follows:

$$s(\mathbf{x}) = \sum_{i=1}^{N} \gamma_i \phi\left(\left\|\mathbf{x} - \mathbf{x}_i\right\|\right) + h(\mathbf{x})$$

The degree of the polynomial has to be chosen depending on the kind of radial function adopted. A radial basis fit exists if the coefficients γ and the weight of the polynomial can be found such that the desired function values are obtained at source points and the polynomial terms gives 0 contributions at source points, that is:

$$s(\mathbf{x}_{k_i}) = g(\mathbf{x}_{k_i}) \quad 1 \le i \le N$$

$$0 = \sum_{i=1}^{N} \gamma_i q(\mathbf{x}_{k_i})$$

for all polynomials q with a degree less or equal than that of polynomial h. The minimal degree of polynomial h depends on the choice of the basis function. An unique interpolant exists if the basis function is a conditionally positive definite function. If the basis functions are conditionally positive definite of order m <= 2, a linear polynomial can be used:

$$h(\mathbf{x}) = \beta + \beta_1 x + \beta_3 y + \beta_4 z$$

The subsequent exposition will assume valid the aforementioned hypothesis. A consequence of using a linear polynomial is that rigid body translations are exactly recovered. The values for the coefficients γ of RBF and the coefficients β of the linear polynomial can be obtained by solving the system:

$$\begin{pmatrix} \mathbf{M} & \mathbf{P} \\ \mathbf{P^T} & \mathbf{0} \end{pmatrix} \begin{pmatrix} \boldsymbol{\gamma} \\ \boldsymbol{\beta} \end{pmatrix} = \begin{pmatrix} \mathbf{g} \\ \mathbf{0} \end{pmatrix}$$

where g are the know values at the source points. M is the interpolation matrix defined calculating all the radial interactions between source points:

$$M_{ij} = \phi\left(\left\|\mathbf{x}_{k_i} - \mathbf{x}_{k_j}\right\|\right) \quad 1 \le i \quad j \le N$$

and P is a constraint matrix that arises balancing the polynomial contribution and contains a column of "1" and the x y z positions of source points in the others three columns:

$$\mathbf{P} = \begin{pmatrix} 1 & x_{k_1}^0 & y_{k_1}^0 & z_{k_1}^0 \\ 1 & x_{k_2}^0 & y_{k_2}^0 & z_{k_2}^0 \\ \vdots & \vdots & \vdots & \vdots \\ 1 & x_{k_N}^0 & y_{k_N}^0 & z_{k_N}^0 \end{pmatrix}$$

Radial basis interpolation works for scalar fields. For the smoothing problem each component of the displacement field prescribed at the source points is interpolated as follows:

$$\begin{cases} v_x = s_x(\mathbf{x}) = \sum_{i=1}^{N} \gamma_i^x \phi\left(\left\|\mathbf{x} - \mathbf{x}_{k_i}\right\|\right) + \beta_1^x + \beta_2^x x + \beta_3^x y + \beta_4^x z \\ v_y = s_y(\mathbf{x}) = \sum_{i=1}^{N} \gamma_i^y \phi\left(\left\|\mathbf{x} - \mathbf{x}_{k_i}\right\|\right) + \beta_1^y + \beta_2^y x + \beta_3^y y + \beta_4^y z \\ v_z = s_z(\mathbf{x}) = \sum_{i=1}^{N} \gamma_i^z \phi\left(\left\|\mathbf{x} - \mathbf{x}_{k_i}\right\|\right) + \beta_1^z + \beta_2^z x + \beta_3^z y + \beta_4^z z \end{cases}$$

Radial basis method has several advantages that make it very attractive in the area of mesh smoothing. The key point is that being a meshless method only grid points are moved regardless of element connected and is suitable for parallel implementation. In fact, once the solution is known and shared in the memory of each calculation node of the cluster, each partition has the ability to smooth its nodes without taking care of what happens outside because the smoother is a global point function and the continuity at interfaces is implicitly guaranteed.

2.3 How does it work

Radial Basis Function interpolation is used to derive the displacement in any location in the space, so it is also available in every grid node.

RBF Morph requires three different steps:

- Step1: [SERIAL] setup and definition of the problem;
- Step2: [SERIAL] solution of the RBF system;
- Step3: [SERIAL/PARALLEL] morphing of surface and volume mesh.

The serial setup requires an intense use of RBF Morph GUI. The GUI offers several tools for the definition of the problem. It is composed by a switchable principal panel (Figure 1). Acting on the radio buttons on the left 8 different operative modes are accessed. The first 4 panels (Config, Encaps, Surfs, Points) are addressed to problem set-up, the other 3 (Solve, Preview, Morph) allows to calculate the rbf solution, to preview its effect and to apply it for morphing and the last panel contains some utilities useful for the RBF Morph software.

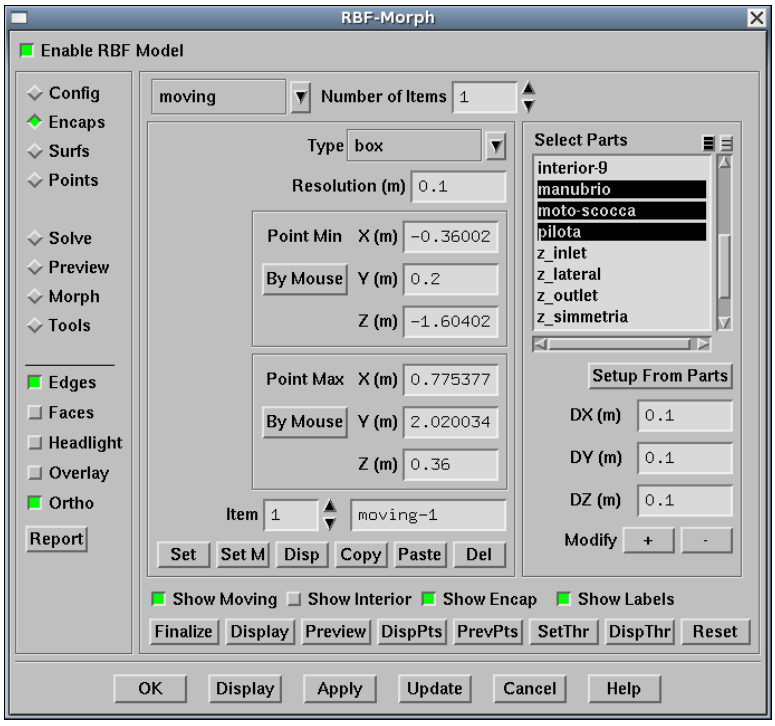

Figure 1: GUI of RBF Morph. The "Encaps" panel is shown

After completing the step1 it is possible to pass to the step2 and calculate the rbf solution. The effect of an imposed modifier can be verified previewing its action (an arbitrary number of surfaces can be morphed on the fly showing the results in the Fluent graphic viewport) without moving the nodes, or exploiting the undo capability that allows to examine the morphed mesh checking its quality and the possible appearing of negative cell volume areas. Once that the modifier is acceptable it can be saved on file. The operation can be repeated for each desired modifier.

The third step can be performed in serial or in parallel with or without the GUI. Once that the solutions are available they can be loaded and used to morph the mesh using the morph panel of the GUI or they can directly used by means of TUI commands that allow to prescribe a single morph or a multi-morph summing the effect of multiple modifiers. Considering that each modifier can be applied with the desired magnitude (i.e. a scalar to set the intensity of the modifier) a parametric Fluent model results.

Since the modifiers are non-linear and large mesh motion are involved the effect of multiple modifier action depends on the application command sequence. For this reason, the multi-morph command superimpose the effects using the same baseline mesh as the starting point of each modifier. Different sequences can be imposed by the user applying the single morph after the action of a previous morph. But in this case a wise procedure is to direct control the effect of the sequence of morphing. For special cases a custom sequence of morphing actions can be programmed as an additional UDF.

3. OPTIMIZATION OF A FSAE CAR AIRBOX

After the Formula ATA event, during a long free-practice session of about 70 laps at "Extrema Kart Speedway" go-kart track (850 meters each lap) located in Modena, some engine functioning irregularities had been traced. A rapid visual exam of the spark plugs (Figure 3b) had shown how the airbox shape together with a changed pressure waves motion due to the new intake and exhaust runners lengths had produced a strong imbalance in the cylinders filling between the external cylinders (1,4) and the internal cylinders (2,3). Being the amount of fuel injected the same for each cylinder (single fueling map), the external cylinders filled with less air encountered some fuel excess conditions (rich mixture, dark electrodes), while the internal ones found less-than-stoichiometric fuel conditions (lean mixture, white electrodes) due to a better exposition to the air flux outgoing from the throttle body.

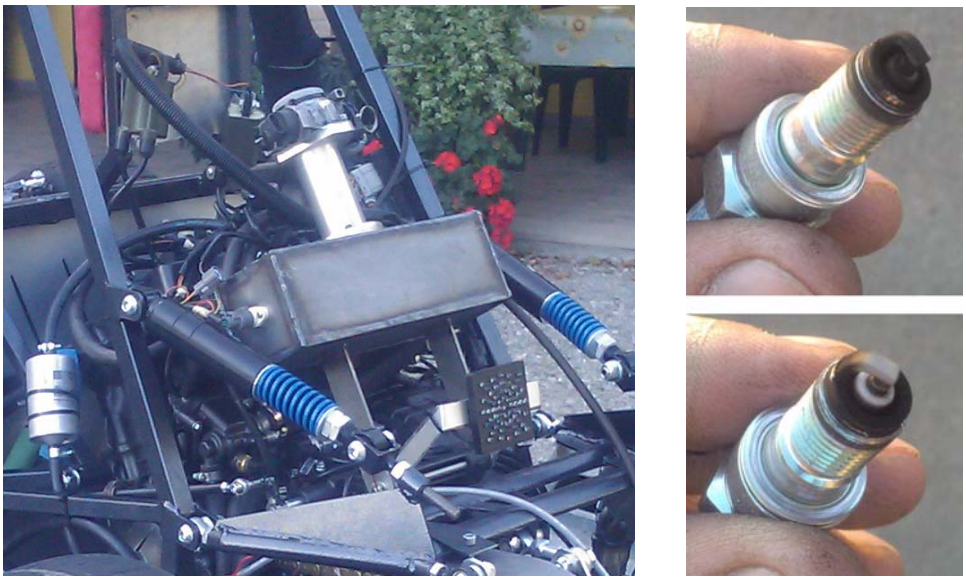

Figure 3: a) The TV-460R air box. b) Spark plugs conditions at the end of the practice session

For this reason it was decided to investigate the problems by means of CFD modeling. The CFD model allowed to predict a consistent mass imbalance between the cylinders (about 10%) completely related to the intake geometric shape.

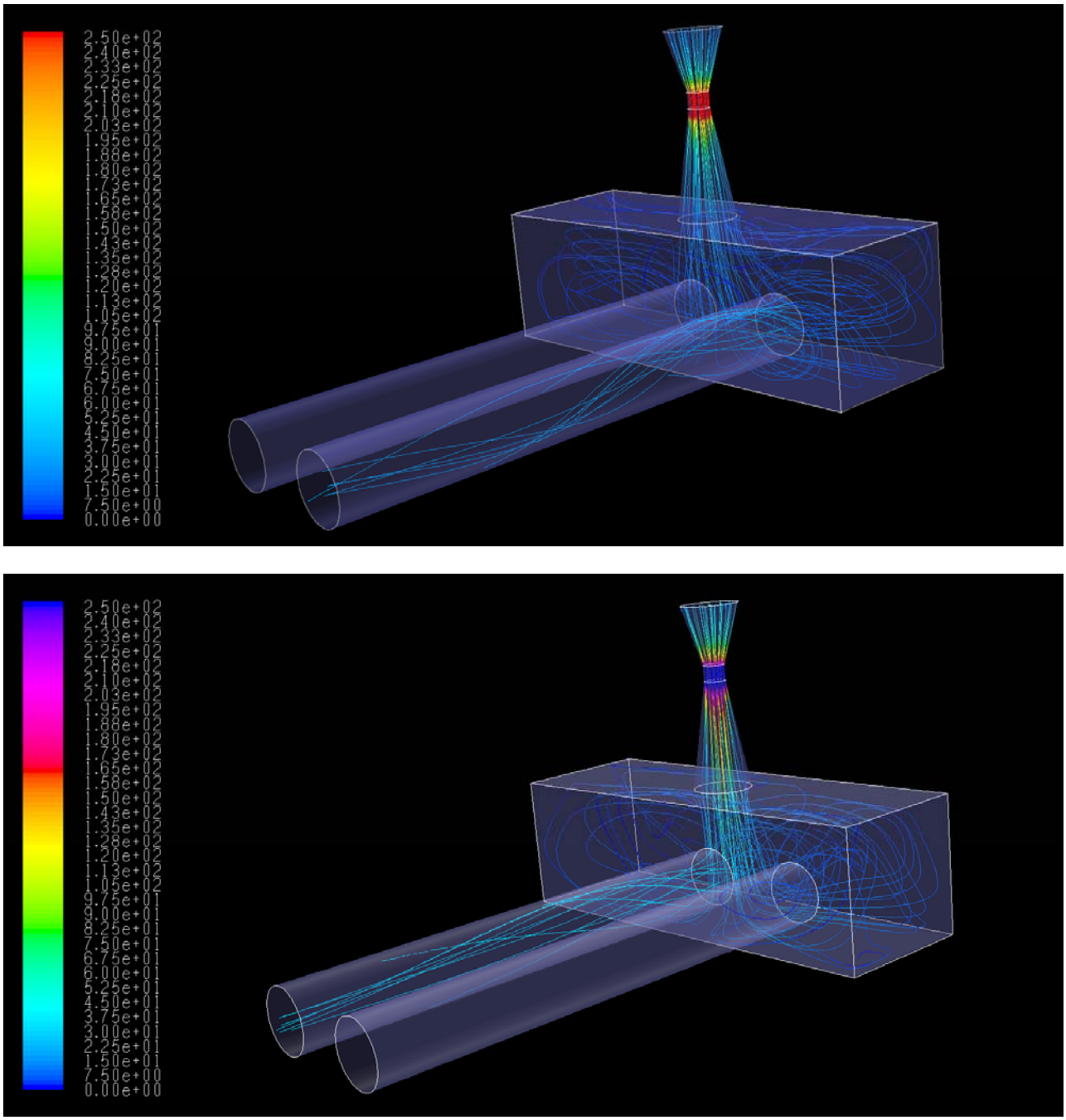

Figure 4: Velocity Magnitude Pathlines inside the fluid domain for the original design a) external runner b) internal runner

3.1 Design of the new baseline solution

The main aim of this work consists in the definition of a new baseline airbox solution on the basis of weakness observed through the CFD analysis of the original shape. Several considerations about the best localization of the restrictor with respect to the airbox position, together with the attempt of keeping the higher possible value for the air density in order to minimize the chocking effect caused by the 20mm restriction imposed by the regulation, suggested the new starting configuration for the airbox (figure 5a).
Everything has to be designed to deal with the regulation constraints about the admitted layout of several mechanical parts, taking into account the external envelop shape of the car.
The new grid is a multi-block structured mesh with non-conformal interfaces at the junction between the restrictor channel outlet and the airbox and between the latter and the runners 1 and 2 (the only ones visualized in the following pictures).

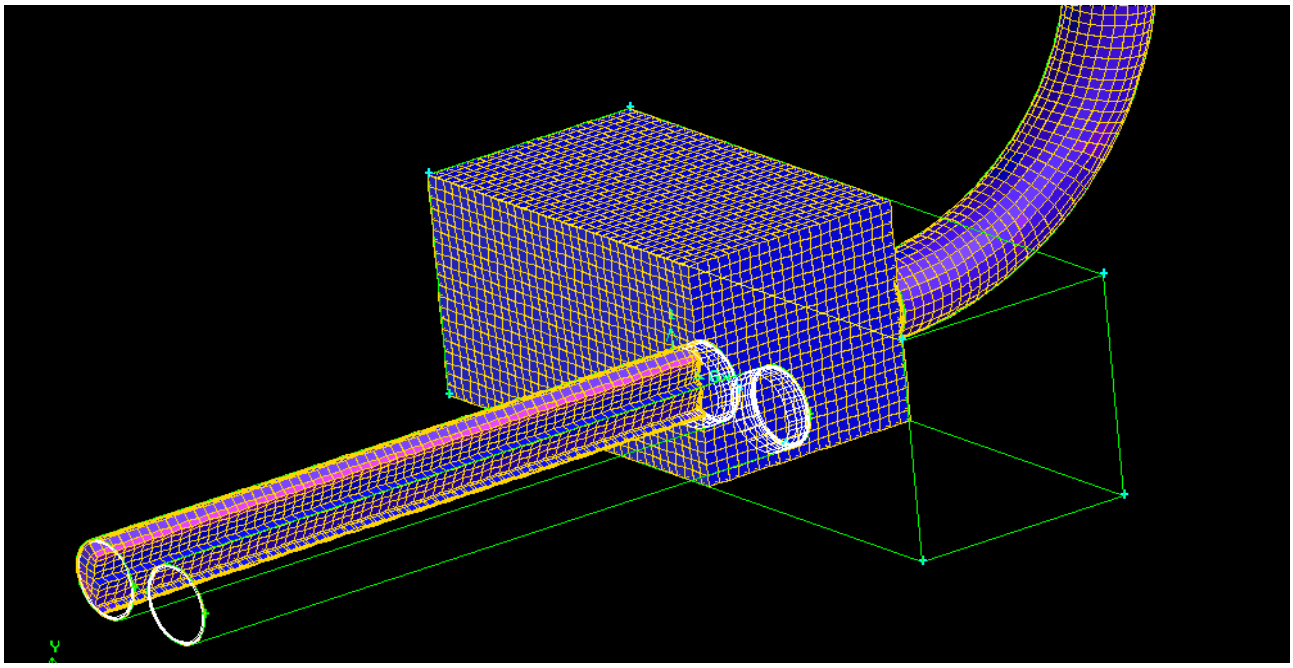

Figure 5: calculation mesh used for the new design.

The airbox volume mesh is completely mapped using regular 0.5 mm hexaedra; the ducts volume mesh is obtained by sweeping the 0.5 mm pave-meshed inlet face along the runner axis path. It brings to a total amount of about 680.000 nodes. The distance of the first nodes in the direction normal to the boundaries is handled with appropriate size functions which allow to obtain the desired values of the quantity y^+ thus permitting a proper behavior of the selected wall functions. The boundary cells are therefore prisms with an aspect ratio bigger than unity (that grows up all the way to the wall) along the streamlines direction.
By inserting the Venturi throat inside the CFD model is possible to have a better control over the flow boundary conditions. A steady state analysis is proposed, so that pressure is not fluctuating with respect to the actual crank angle: it means that the pressure values are calibrated to maintain a desired velocity in the throat. For example, depression values that bring over the sonic limit are not taken into account because the car will be tuned in order to not reach such conditions. Different flow conditions are simulated: from the ones characterized by a low velocity in which turbulence dissipation has a little importance to the almost transonic ones where choking begins to appear and the critical conditions of the cylinder filling are almost reached.
Once the depression values had been set up, the baseline model passed to the morpher was simplified by eliminating the restrictor fluid zone and substituting it with a constant-section duct. In this way calculation becomes easier: lower compressible effects are taken into account, less stiff iterative equations are solved; despite of this, similar flow conditions are generated at the restrictor duct exit,

thus producing the same behavior during the deceleration of the fluid vein while crossing the airbox. It resulted in a faster convergence and in shorter computation times to loop over the multiple configurations investigated by the morpher tool. However, through retaining this same condition in all cases, the general trend is not affected.
The boundary conditions are pressure inlet at restrictor inlet with a static pressure set to the atmospheric value; pressure outlet at runners 1 and 2 outlets with variable pressure values depending on the simulated case. The solver is a pressure-based one; interfaces properties are calculated through Green-Gauss cell based interpolation; the solution is iterative and steady; the flux is compressible; turbulence effects are taken into account using a standard k-ε model; the discretization of energy and momentum equations is ruled by a third order MUSCLE method provided to minimize false diffusion and thus a freezing effect over the incoming flow, while the pressure correction equation is solved with a PRESTO! method. All these settings are retained to have a better comparison between the morphed geometries, in order to exclude discretization-connected errors between them. Convergence is gained with a few iterations for both obtaining low residuals and stabilized quantity at runner outlets: about 300 iterations are needed for the former, around 1000 for the latter. Required residuals are 10^{-3} for the continuity equation and the turbulence parameters, 10^{-5} for the momentum equations and 10^{-6} for the energy equations. The authors had deem the mass flow outlet throughout the runner outlet section converged when only changes to the 4^{th} decimal digit appeared.

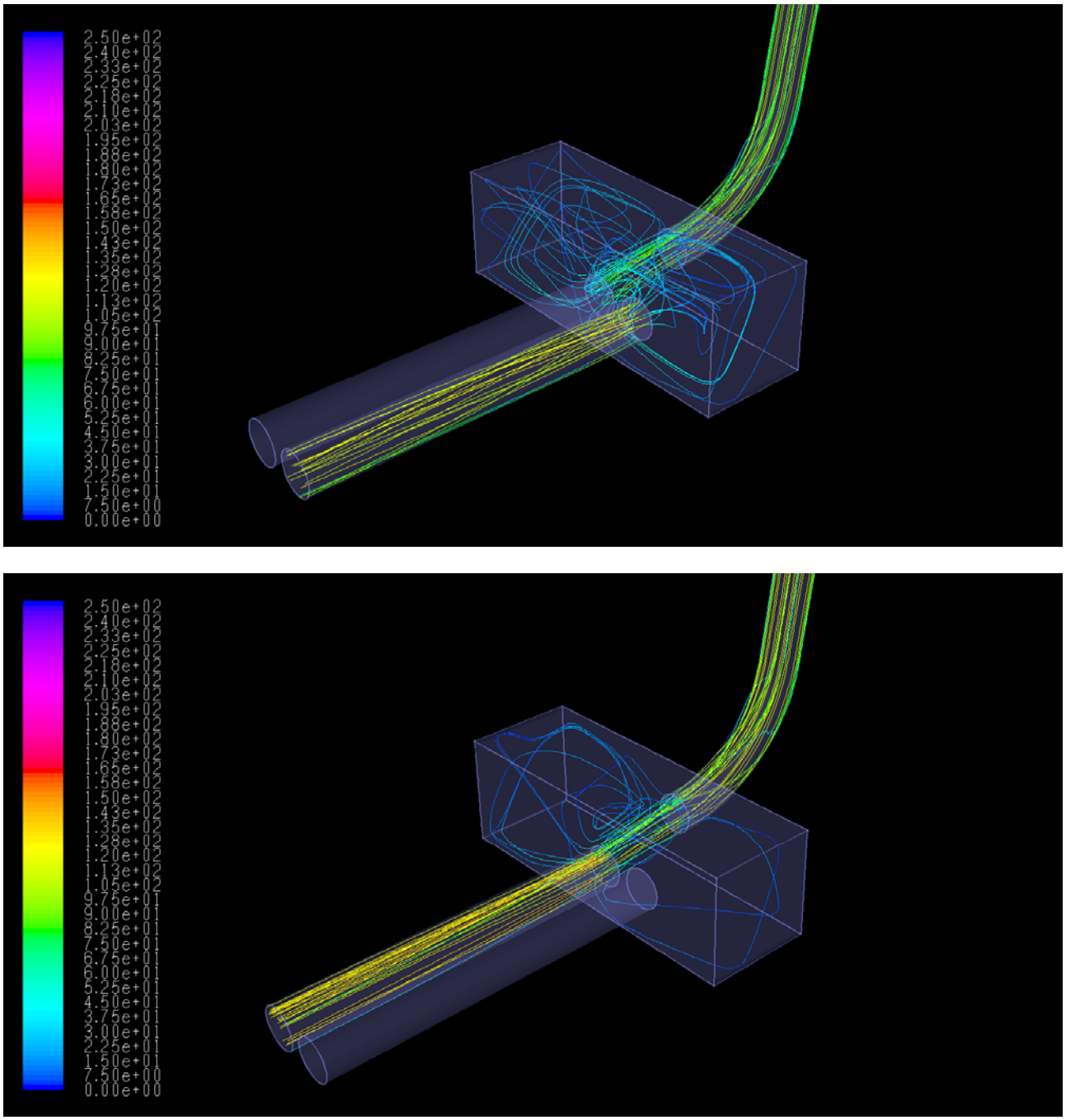

Figure 6: Velocity Magnitude Pathlines inside the fluid domain for the new design in the baseline configuration a) external runner b) internal runner.

3.2 Parameterisation of the new solution by mesh morphing

The RBF Morph add-on has been used to deform the CFD model of the new geometry considering three deforming actions:

- changing the width of the airbox;
- tapering the airbox changing the width of the airbox at the throttle side;
- changing the depth width of the air box.

All the morphing actions and their combinations produce a shape that fit the room available and so are compliant with the packaging constraint.

Aforementioned shape modifiers effects is highlighted in figure 7 where all the actions are imposed to the model (using the middle level intensity) and the resulting shape (7 right) is compared with the baseline shape (7 left).
To better understand the effect of each modifier two levels of amplifications of each parameters are used separately and resulting shape are exposed in Figure 8, 9 and 10. Note that for convenience of understanding of the pictures, the current amplification list is part of the image and is located at the left-bottom side of each image.

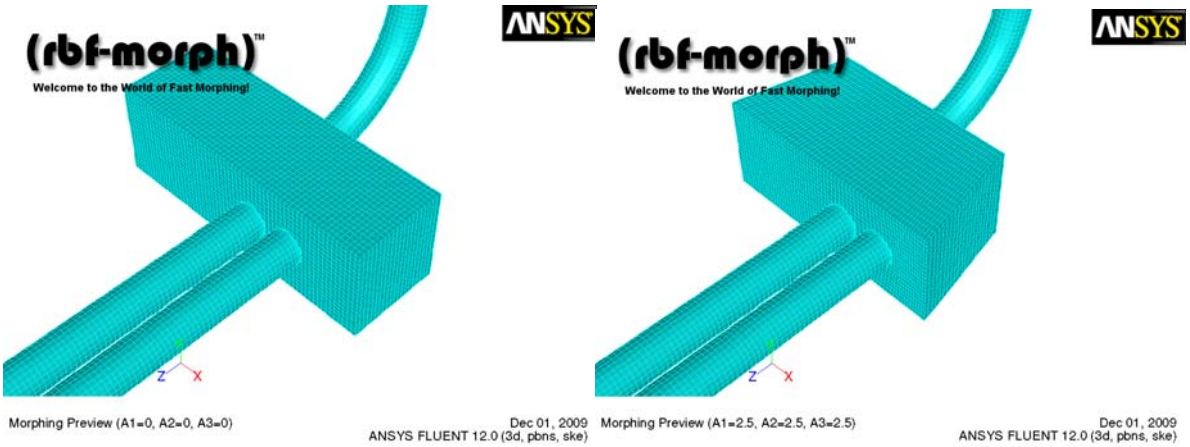

Figure 7: Original mesh (left) and morphed mesh using the action of all the modifiers in the middle level intensity.

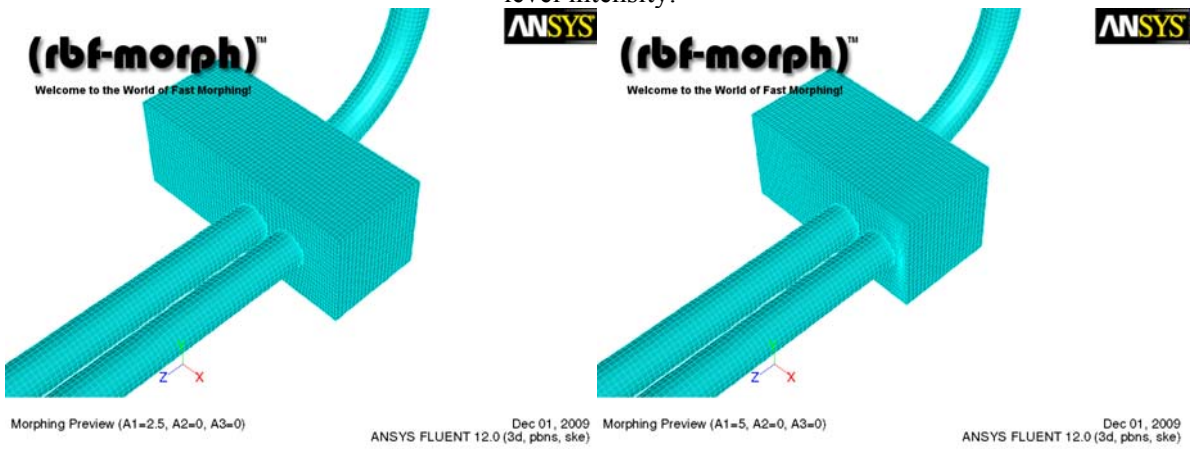

.

Figure 8: The mesh is morphed to change the width of the air box (two levels shown corresponding to a change of 2.5 cm and 5 cm).

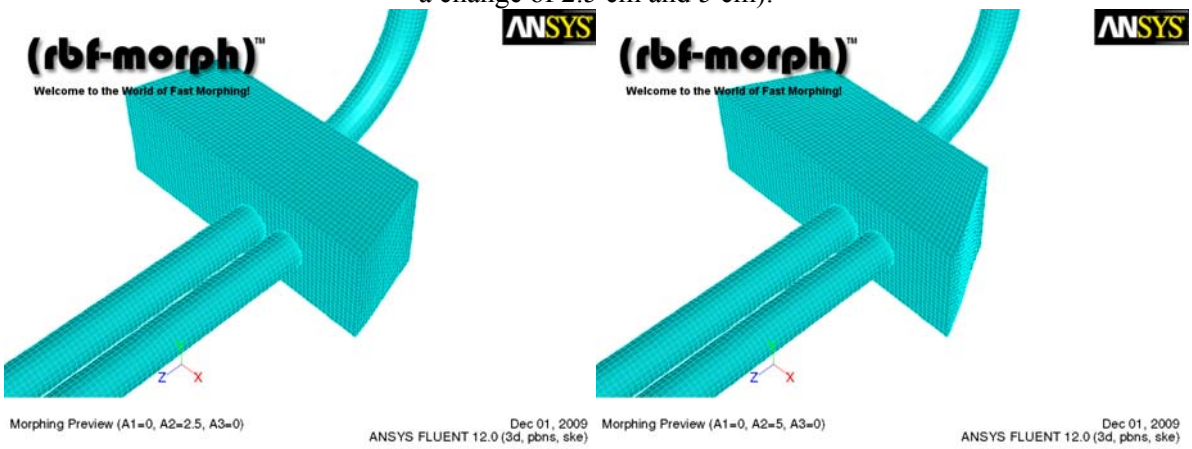

Figure 9: The mesh is morphed to taper the air box changing the width of the air box at the throttle side (two levels shown corresponding to a change of 2.5 cm and 5 cm).

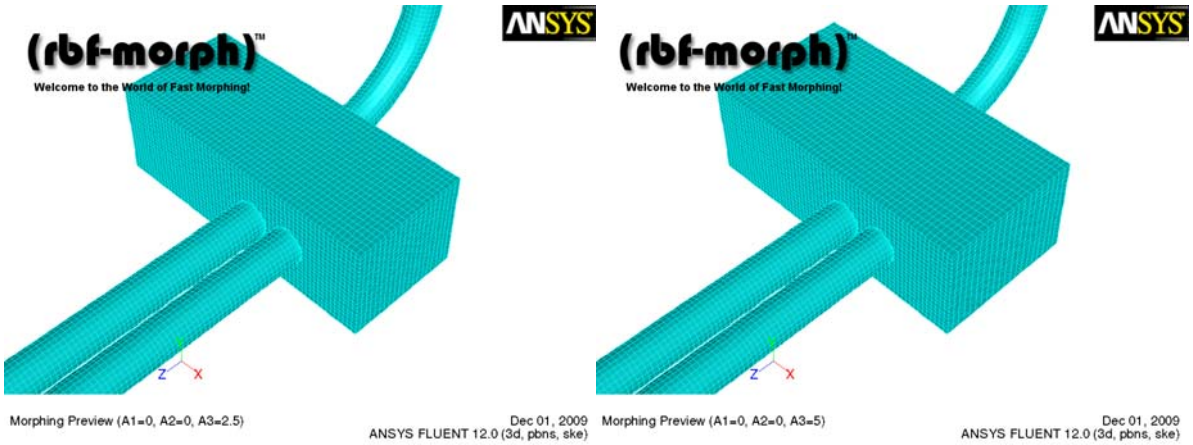

Figure 10: The mesh is morphed to change the depth of the air box (two levels shown corresponding to a change of 2.5 cm and 5 cm).

3.3 Optimisation results

After having proved the imbalance in the fresh charge flowing inside the runners 1 and 2, a new baseline configuration has been created for the airbox. How figures 4a and 4b clearly show, an higher number of visualized pathlines inside the intake ducts and a lighter color of these streamlines with respect to figures 3a and 3b stand for a better filling and a bigger mass flow rate.
Despite of this, some differences in the flow field can be easily observed between figures 4a and 4b. When the intake valves at the end of the external runner are opened a more developed vorticity is generated: some of the streamlines are directly sent against the wall represented by the plate in front of the restrictor outlet, where they are 'reflected' behind; some others are trapped inside the opened duct. When the internal runner is opened the most part of the pathlines (almost all of them) enter inside the runner inlet, having not yet dissipated the whole kinetic energy. Thus the aforementioned not desired effect of a non homogeneous filling is still present (baseline solution for the new configuration are reported in the case 1 of Table 3).
Starting now from a better configuration, the RBF Morph can be used as a powerful tool to optimize the airbox geometry; 27 geometry had been investigated using the shape parameters previously described according to the DOE factorial space reported in Table 2. All the calculations over the new shapes configurations are performed using a single case file and a script that automates the morphing and store results in a proper folder tree. Such parametric analysis is generated by means of a single click command available in RBF Morph 1.2 that allows to generate the folder tree (one folder for each DOE point), the symbolic links between reference files (i.e. fluent case and one configuration and solution file for each shape modifier) and a patched version of the user journal file in which the correct shape is invoked using the TUI command:

```
(rbf-morph '(("sol-1" amp-1) ("sol-2" amp-2)...("sol-n" amp-n)))
```

where the correct amplifications (amp-1, amp-2,.., amp-n) of the DOE point are patched. Each solution is controlled in batch using a standard journal file; among the output results stored is included also the mass flow rates through the two simulated runners for two different run (switching the opening between the two runners). Results obtained for each DOE point are summarized in Table 3.

Table 2: Full factorial DOE Design space.

	deltax-1cm	deltax-outlet-1cm	deltaz-1cm
1	0	0	0
2	2,5	0	0
3	5	0	0
4	0	2,5	0
5	2,5	2,5	0
6	5	2,5	0
7	0	5	0
8	2,5	5	0
9	5	5	0
10	0	0	2,5
11	2,5	0	2,5
12	5	0	2,5
13	0	2,5	2,5
14	2,5	2,5	2,5
15	5	2,5	2,5
16	0	5	2,5
17	2,5	5	2,5
18	5	5	2,5
19	0	0	5
20	2,5	0	5
21	5	0	5
22	0	2,5	5
23	2,5	2,5	5
24	5	2,5	5
25	0	5	5
26	2,5	5	5
27	5	5	5

Table 3: DOE Analysis results, mass flow (kg/s) and relative imbalance (%).

	runner1	runner2	imbalance	average	relative imbalance
1	0,1087	0,1222	0,0135	0,1155	-5,9
2	0,1090	0,1216	0,0126	0,1153	-5,5
3	0,1112	0,1205	0,0094	0,1158	-4,0
4	0,1086	0,1227	0,0141	0,1156	-6,1
5	0,1091	0,1248	0,0158	0,1169	-6,7
6	0,1102	0,1240	0,0138	0,1171	-5,9
7	0,1094	0,1221	0,0127	0,1157	-5,5
8	0,1101	0,1238	0,0137	0,1170	-5,8
9	0,1108	0,1238	0,0129	0,1173	-5,5
10	0,1097	0,1183	0,0086	0,1140	-3,8
11	0,1095	0,1187	0,0091	0,1141	-4,0
12	0,1110	0,1212	0,0102	0,1161	-4,4
13	0,1093	0,1203	0,0110	0,1148	-4,8
14	0,1111	0,1214	0,0103	0,1163	-4,4
15	0,1107	0,1235	0,0127	0,1171	-5,4
16	0,1101	0,1228	0,0127	0,1165	-5,4
17	0,1114	0,1236	0,0122	0,1175	-5,2
18	0,1114	0,1240	0,0126	0,1177	-5,4
19	0,1102	0,1172	0,0069	0,1137	-3,0
20	0,1112	0,1205	0,0093	0,1159	-4,0
21	0,1118	0,1173	0,0055	0,1145	-2,4
22	0,1110	0,1197	0,0088	0,1154	-3,8
23	0,1109	0,1134	0,0025	0,1122	-1,1
24	0,1110	0,1125	0,0015	0,1117	-0,7
25	0,1109	0,1185	0,0076	0,1147	-3,3
26	0,1116	0,1123	0,0007	0,1119	-0,3
27	0,1120	0,1144	0,0023	0,1132	-1,0

Optimal points can be obtained using the response surface technique. A custom MathCAD implementation has been used for this purpose. The original dataset of true calculated points is used to generate a meta model of the system. The RBF method is chosen to extrapolate the system response using a cubic function ($\phi(r)=r^3$). The theoretical background of RBF is the same already exposed for the morpher because the design space has 3 dimensions; in this case only two scalar functions are extrapolated (i.e. mass imbalance and overall mass flow); however such approach can be easily extended to the general case of n input parameters and m output responses. Thanks to the meta model a new extrapolated full factorial data set is generated in a few seconds. All the results are then represented in a plot that allows to find the Pareto optimal curve. In figures 11 and 12 all original solution points are plotted together with the new extrapolated dataset. Two optimal solutions are highlighted. The first one, shown in Figure 11 is the one that gives the minimum imbalance; the second one, shown in Figure 12 is the one that gives the maximum delivered mass flow with the constraint of a maximum imbalance equal to 2%. The CFD results for proposed solutions are represented in Figures 13 and 14.

$$Xop := Bigset_{IDopt,6} = 0.112 \qquad \begin{pmatrix} \delta_x \\ \delta_{xout} \\ \delta_z \end{pmatrix} := \begin{pmatrix} Bigset_{IDopt,2} \\ Bigset_{IDopt,3} \\ Bigset_{IDopt,4} \end{pmatrix} = \begin{pmatrix} 3.25 \\ 4.25 \\ 5 \end{pmatrix}$$

$$Yop := Bigset_{IDopt,5} = -0.156$$

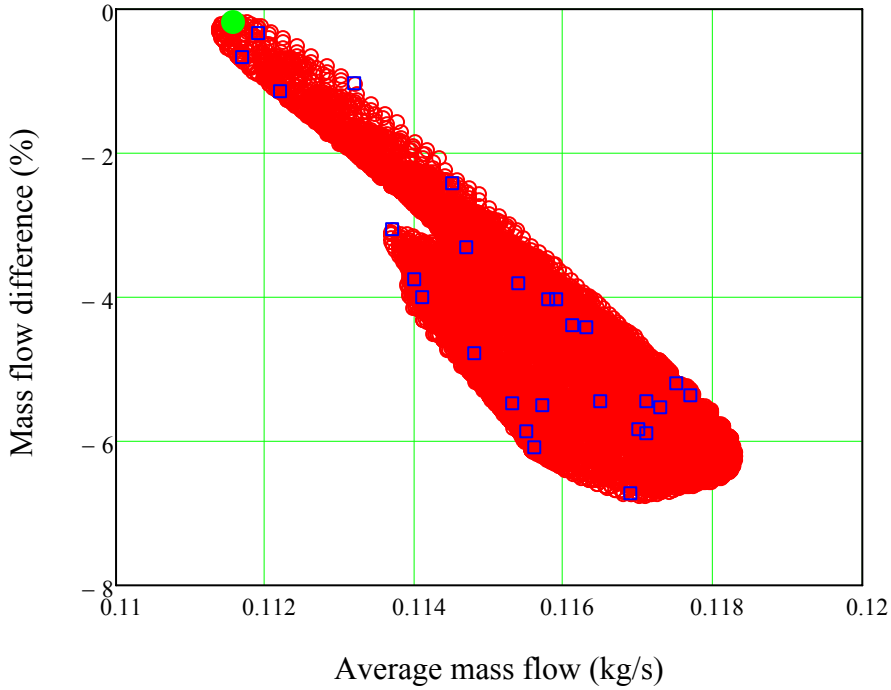

Figure 11: response of the system for the original dataset and the extrapolated one, minimum imbalance point highlighted.

$$Xop := Bigset_{IDopt,6} = 0.114 \qquad \begin{pmatrix} \delta_x \\ \delta_{xout} \\ \delta_z \end{pmatrix} := \begin{pmatrix} Bigset_{IDopt,2} \\ Bigset_{IDopt,3} \\ Bigset_{IDopt,4} \end{pmatrix} = \begin{pmatrix} 4.75 \\ 5 \\ 4.5 \end{pmatrix}$$

$$Yop := Bigset_{IDopt,5} = -1.95$$

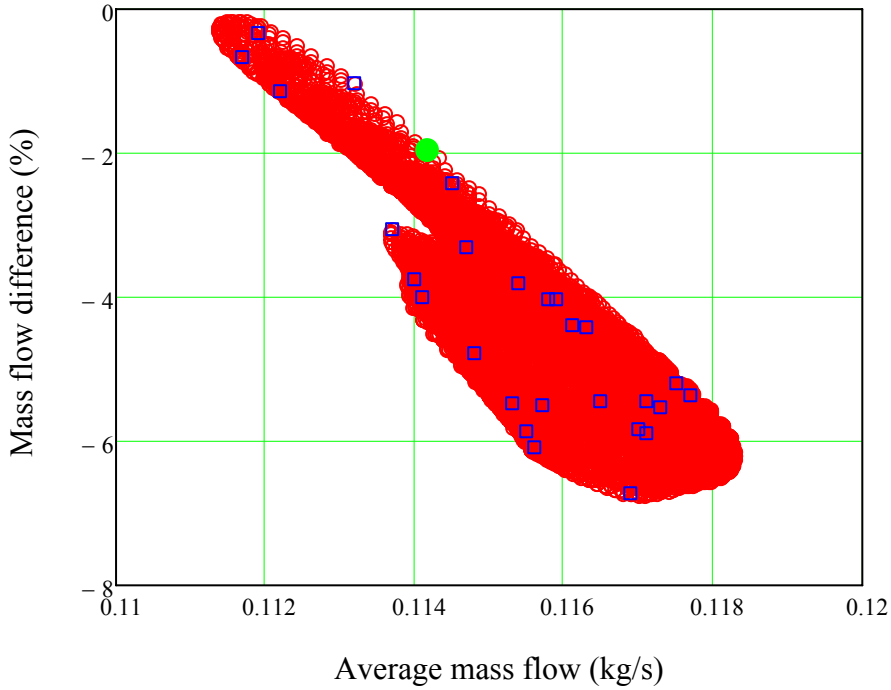

Figure 12: response of the system for the original dataset and the extrapolated one, 2% imbalance point highlighted.

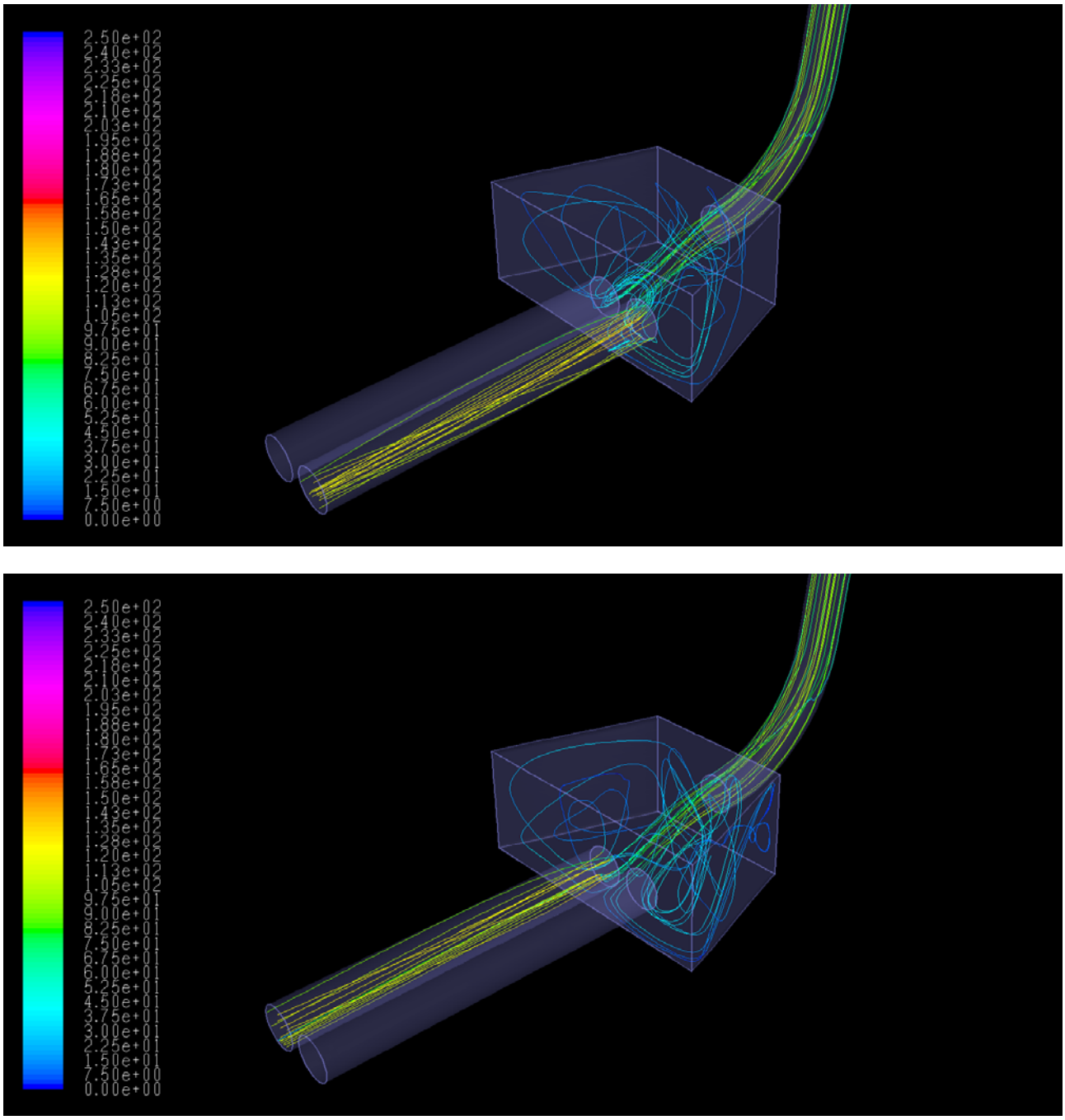

Figure 13: Velocity Magnitude Pathlines inside the fluid domain for the new design in the minimum imbalance configuration a) external runner b) internal runner.

The internal runner is not well served as in the previous configuration; many streamlines are not directly going inside the central ducts and are reflected behind creating two big counter-rotating vortexes inside the airbox. Accordingly to this, anyway, the desired effect of reducing the imbalance is gained, also if a lower mass flow comes out from it.

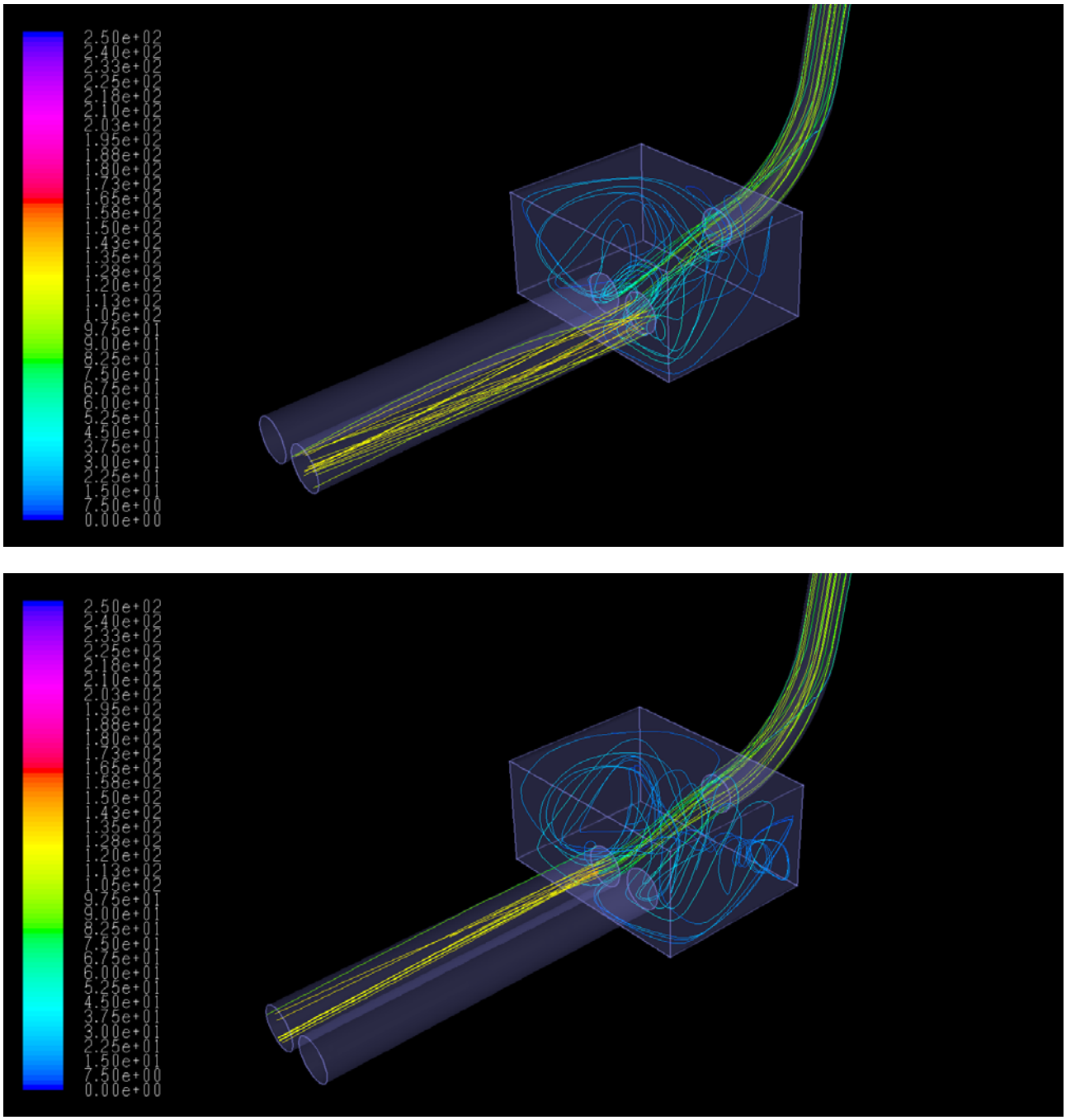

Figure 14: Velocity Magnitude Pathlines inside the fluid domain for the new design in the 2% imbalance configuration a) external runner b) internal runner.

The same effects outlined above are shown. By the way, an increment of 2.33% is obtained in front of a loss of homogeneity of about 1.7%.

4. CONCLUSIONS

In this paper the application of RBF Morph tool for the CFD optimisation of a FSAE car airbox has been presented. The tool has proven to be very useful for industrial applications and has allowed to successfully manage all the desired configurations.

The intake system optimization process is still ongoing. Further improvements as a new length for the intake ducts, a partial bending of the runners, a new exhaust system and an unsteady simulation of the flux will be analyzed in the future by taking into account the 1-D non stationary effects.

An experimental testing campaign will be arranged to have a direct numerical-experimental comparison for the new CFD models.

5. REFERENCES

[1] RBF Morph web portal: www.rbf-morph.com.
[2] M.E. Biancolini; C. Biancolini; E. Costa; D. Gattamelata; P.P. Valentini, Industrial Application of the Meshless Morpher RBF Morph to a Motorbike Windshield Optimisation, European Automotive Simulation Conference (EASC), 6-7 July 2009, Munich, Germany.
[3] Tor Vergata Karting web portal (in Italian): www.torvergata-karting.it
[4] M. E. Biancolini , "Engine/vehicle matching for a FSAE race car", 14th Asia Pacific Automotive Engineering Conference 07APAC-229.